

# Structural Permutation of Potent Cytotoxin, Polytheonamide B: Discovery of Cytotoxic Peptide with Altered Activity

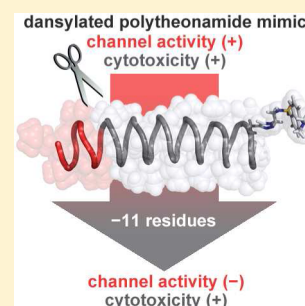
Hiroaki Itoh and Masayuki Inoue\*

Graduate School of Pharmaceutical Sciences, The University of Tokyo, Hongo, Bunkyo-ku, Tokyo 113-0033, Japan

## Supporting Information

**ABSTRACT:** Polytheonamide B (**1**) is an ion-channel forming natural peptide with a D,L-alternating 48 amino acid sequence, which is an exceedingly potent cytotoxin. We recently designed and synthesized a simplified dansylated polytheonamide mimic **2**, in which six amino acid residues were modified from **1**, and demonstrated that **2** emulated the functions of **1**. Here we report a comprehensive structure–activity relationship study of substructures of **2**. A unified synthetic strategy was developed for highly automated syntheses of 13 peptide sequences of 27 to 39 amino acid residues, and the artificial 37-mer peptide **6** was discovered to be significantly more toxic than the other 12 compounds toward P388 mouse leukemia cells ( $IC_{50} = 3.7$  nM). Ion exchange activity experiments of **6** using the liposome and P388 cells both demonstrated that **6** did not possess ion-channel activity, strongly suggesting that **6** exerted its potent cytotoxicity through a distinct mode of action from **1** and **2**.

**KEYWORDS:** Cytotoxic agents, natural products, structure–activity relationships, solid-phase synthesis, synthetic ion channels



Polytheonamide B (**1**, Figure 1) is a giant natural peptide (MW 5030) and a potent cytotoxic agent ( $IC_{50} = 0.098$  nM, mouse leukemia P388 cells).<sup>1,2</sup> Linearly aligned residues of **1** with alternating D- and L-chiralities consist of 13 non-proteinogenic and 6 proteinogenic amino acids, and S,S-dimethyl-2-oxohexanoate (Ncap) at the N-terminus. The secondary structure of **1** is reported to be a 45 Å-long  $\beta^{6,3}$ -helix,<sup>3</sup> which is believed to function as a transmembrane ion channel. In fact, monomeric **1** was shown to selectively transport monovalent cations (e.g.,  $H^+$ ,  $Na^+$ ,  $K^+$ ) across the membrane,<sup>4,5</sup> while the structurally related gramicidin D (**3**)<sup>6,7</sup> must form a head-to-head dimer to act as a similar channel. The exceedingly high toxicity of **1** has been attributed to its ability to efficiently form a highly stable ion channel.

We recently reported the total synthesis of polytheonamide B (**1**), which involved 161 total steps from commercially available materials.<sup>8–10</sup> Subsequent biological evaluations of the substructure<sup>11</sup> and N-terminal derivatives of **1** provided valuable information on the structural elements relating to the function of **1**.<sup>12</sup> However, the length of the total synthesis limited the supply of **1** to perform further systematic structure–activity relationship (SAR) studies.

To overcome this issue, we designed an artificial ion channel molecule, designated as dansylated polytheonamide mimic **2**.<sup>13</sup> The structure of **1** was simplified by removing or changing the  $\beta$ -substituents of residues 2, 22, 29, 37, and 47, and the dansylated amino acid was placed at residue 44 as a reporter of the localization of **2**. Compound **2** not only required significantly fewer synthetic steps in comparison to original **1** (127 steps vs 161 steps) but also successfully exhibited potent cytotoxicity toward P388 mouse leukemia cells ( $IC_{50} = 12$  nM) and displayed  $H^+$  and  $Na^+$  ion channel activities. Therefore, it is

evident that **2** can emulate the functions of **1** despite structural modifications at six amino acid residues of **1**.

In the total synthesis of the 48-residue sequence **2**, assembly of the D,L-alternating 37 amino acid sequence from residues 12 to 48 was realized through a single automatic solid-phase synthesis. Synthesis of compound **2** was completed via dansyl group introduction, one fragment-coupling reaction between residues 11 and 12 and global deprotection. The optimized solid-phase synthesis technology permitted us to initiate a program directed toward efficient automated preparation of various sequences of **2** in the search for biologically active compounds with minimum molecular complexity. Herein we report the chemical synthesis of 13 substructures of polytheonamide mimic **2**, which resulted in the discovery of a compound of 37 amino acid residues with nanomolar level toxicity ( $IC_{50} = 3.7$  nM), along with five submicromolar level cytotoxins, and distinct activities between natural product **1**, mimic **2**, and the 37-mer fragment of **2**.

The 13 N-terminal peptides **4–16** (H-[X-48]-OH, X = 10–22) were targeted for comprehensive SAR studies (Table 1). These sequences were designed to be elongated only by automatic solid-phase synthesis, in that the compounds do not possess sterically demanding  $\beta$ -methyl valines (residues 2, 4, 5, 6, 8, 9), which significantly decrease the condensation yields.

The synthesis of all the compounds **4–16** was started from H-Thr(*t*-Bu)-2-chloro trityl resin **17**<sup>14,15</sup> using Fmoc-based solid-phase peptide synthesis.<sup>16</sup> To maximize the overall yield, a powerful reagent system HATU/HOAt<sup>17</sup> was applied for condensation of the amino acids, and *t*-Bu, Tr, and Tmb were

Received: September 1, 2012

Accepted: November 1, 2012

Published: November 1, 2012

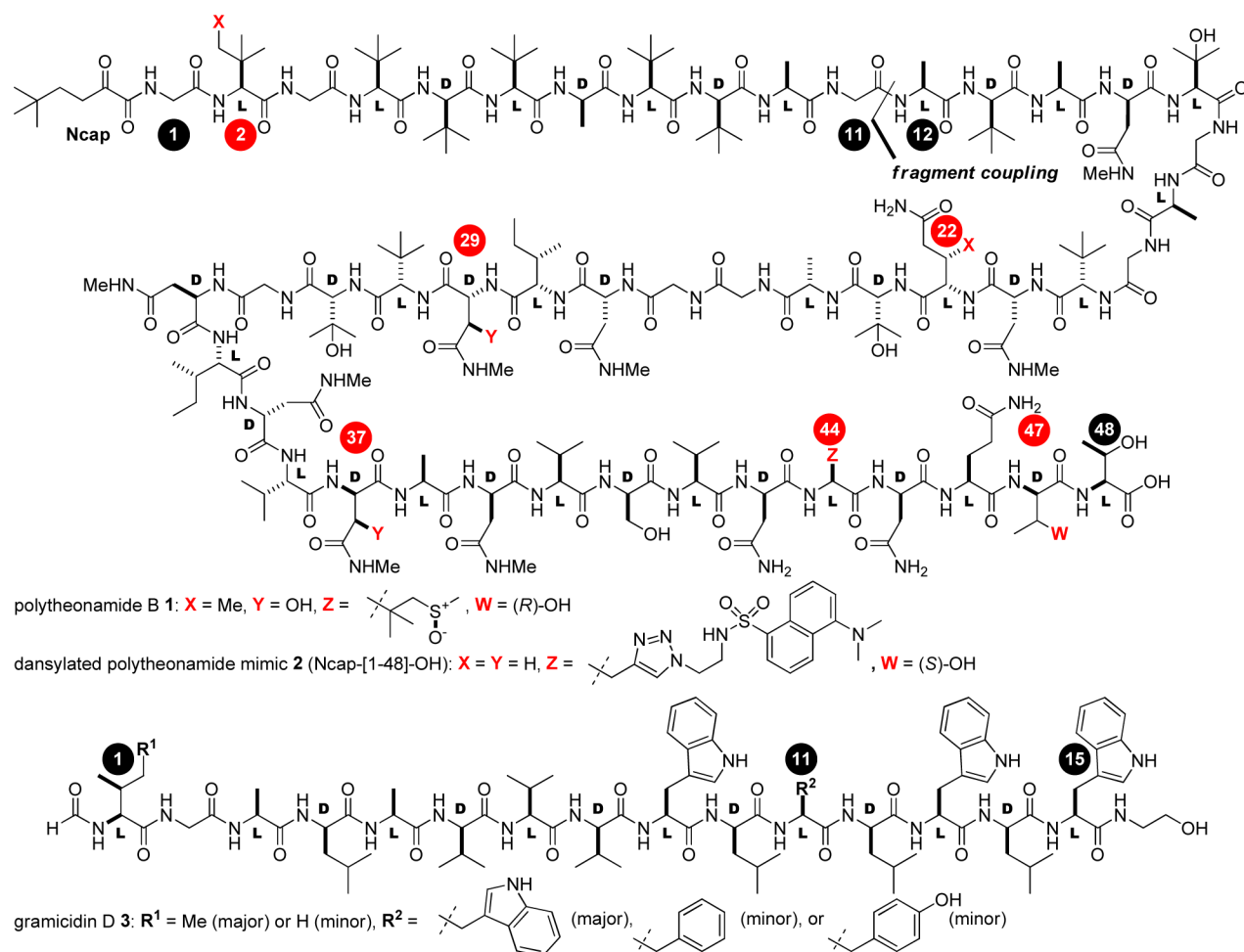


Figure 1. Structures of polytheonamide B, dansylated polytheonamide mimic, and gramicidin D.

Table 1. Overall Yields and Cytotoxicity Data of the Synthesized Peptides<sup>a</sup>

compd	overall yield from 17 (%)	IC <sub>50</sub> <sup>a</sup> (nM)
1: polytheonamide B		0.098
2: Ncap-[1-48]-OH		12
3: gramicidin D		4.3
4: H-[10-48]-OH	0.30	>420
5: H-[11-48]-OH	0.20	>420
6: H-[12-48]-OH	0.07	3.7
7: H-[13-48]-OH	0.10	81
8: H-[14-48]-OH	0.09	100
9: H-[15-48]-OH	0.17	>420
10: H-[16-48]-OH	0.14	140
11: H-[17-48]-OH	0.14	>450
12: H-[18-48]-OH	0.14	190
13: H-[19-48]-OH	0.18	>410
14: H-[20-48]-OH	0.32	390
15: H-[21-48]-OH	0.28	>250
16: H-[22-48]-OH	0.10	>420

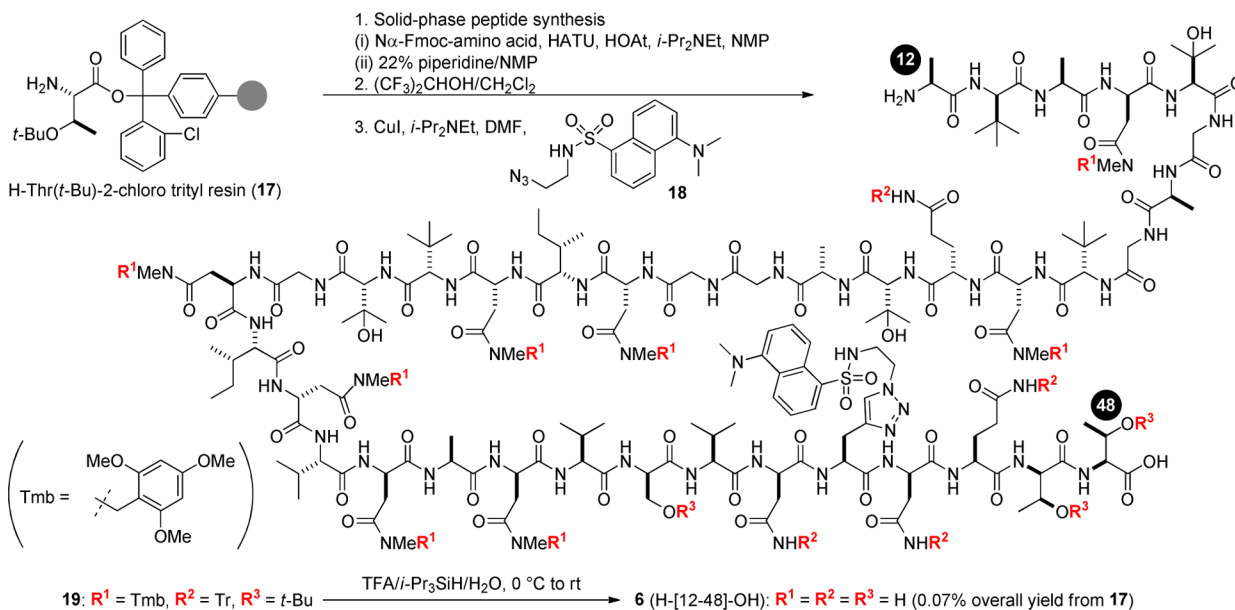
<sup>a</sup>IC<sub>50</sub> values were determined from the results of growth inhibition assays (XTT method) performed on P388 mouse leukemia cells.

used as the protective groups for the hydroxy, primary amide, and methyl amide functionalities of the side chains, respectively. The synthetic route to **6** (H-[12-48]-OH) is illustrated as a representative example in Scheme 1. After stepwise assembly of

the 36 monomers, the peptide was cleaved from the 2-chloro trityl resin under mild acidic conditions [(CF<sub>3</sub>)<sub>2</sub>CHOH/CH<sub>2</sub>Cl<sub>2</sub> = 1:3] and purified with HPLC, and then the dansyl moiety **18**<sup>18</sup> was incorporated into the alkyne group of residue 44 via 1,3-dipolar addition,<sup>19–22</sup> giving rise to **19**. Finally, simultaneous removal of the side chain protective groups (the eight Tmb,<sup>23</sup> four Tr, and three *t*-Bu groups) from **19** in TFA/*i*-Pr<sub>3</sub>SiH<sup>24</sup>/H<sub>2</sub>O (95:2.5:2.5) successfully delivered **6** (0.07% overall yield from **17** after HPLC purification). Synthesis of **6** required 98 total steps, comprising 73 steps of the solid-phase synthesis and 25 steps of the solution-phase synthesis (monomer syntheses, dansyl introduction, and global deprotection), demonstrating the highly automated nature of the strategy. Most importantly, the developed procedure was applicable for efficient preparations of longer **4–5** and shorter **7–16** in a unified fashion (0.1–0.3% overall yields, Table 1).

A collection of the analogues **4–16** allowed us to determine the cytotoxicities of this series toward P388 mouse leukemia cells (Table 1).<sup>25,26</sup> Six out of 13 compounds showed detectable toxicities, and submicromolar level activities (IC<sub>50</sub> = 81–390 nM) were observed for five of them (**7**, **8**, **10**, **12**, and **14**). Surprisingly, compound **6** (H-[12-48]-OH) was found to be at least 20-fold more toxic (IC<sub>50</sub> = 3.7 nM) than the other 12 analogues, and its toxicity was even 3 times higher than that of the longer polytheonamide mimic **2** (Ncap-[1-48]-OH; IC<sub>50</sub> = 12 nM) and comparable to that of gramicidin D **3** (IC<sub>50</sub> = 4.3 nM). It is worthy to note that a drastic increase

## Scheme 1. Representative Synthetic Scheme of the Substructures of 2



in potency was observed when only one amino acid was detached from 5 (H-[11–48]-OH) or attached to 7 (H-[13–48]-OH). These results strongly suggested the significance of the specific structure of 37-mer 6 for the potent cytotoxicity.

A key question was whether this new cytotoxic agent 6 shared the same mechanism of action as the parent natural product 1, mimic 2 and gramicidin D 3. Since 1–3 are known to form ion channels in lipid bilayers, the ion transport activity of 6 was compared to those of 1–3 using liposomes, which are models of cell membranes (Figure 2). The liposomes were

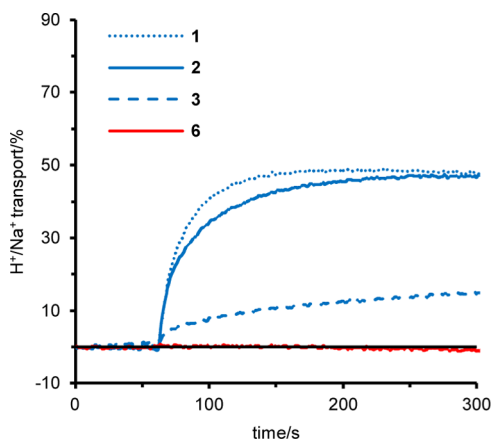


**Figure 2.** Time-course of  $\text{H}^+/\text{Na}^+$  exchange across lipid bilayers of pH-gradient liposomes (EYPC/cholesterol = 2:1) caused by 1, 2, 3, and 6. The ion transport was evaluated as the pH-dependent fluorescence from pyranine standardized against the maximum exchange by Triton X-100. In all the experiments, the peptides were added at 60 s.

prepared in HEPES buffer containing 200 mM NaCl with a pH gradient, a pH of 6.5 inside the liposome, and a pH of 7.5 outside. A fluorescent pH indicator, pyranine, was incorporated in the liposomes.<sup>27,28</sup> Addition of the peptide channels (125 nM) then permitted exchange between protons and  $\text{Na}^+$  ions across the lipid bilayer of the vesicles to preserve the ionic milieu, leading to a fluorescence increase caused by deprotonation of pyranine. In contrast to the cases of 1, 2,

and 3, which all induced an increase of the fluorescence over time through the  $\text{H}^+/\text{Na}^+$  exchange, addition of peptide 6 resulted in no change. The lack of effect of 6 on the liposome membranes demonstrated that it had no ion transport activity or no membrane disruption activity in this assay.<sup>29–31</sup>

To further investigate that 6 has a different activity from the ion channel forming natural products 1 and 3, an ion exchange assay was performed using the P388 cells, toward which 1, 3, and 6 all exhibited strong toxicities. In this assay, membrane permeable BCECF-AM 20 (Figure 3) is externally applied to

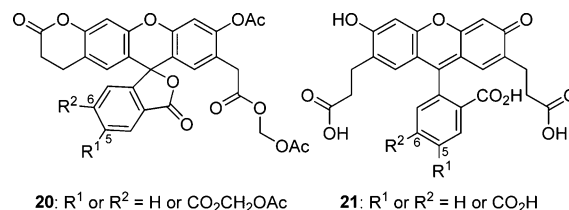


**Figure 3.** Structures of BCECF-AM (20) and BCECF (21).

the P388 cells, and esterase-mediated hydrolysis of the ester moieties of 20 selectively occurs within the cell membranes to lead to encapsulation of a hydrophilic pH indicator, BCECF 21.<sup>32</sup> Next, the resultant cells are suspended in pH 7.8 MOPS buffer containing 130 mM NaCl to apply a  $\text{Na}^+$  gradient, and treated with the peptides (125 nM) to measure the ion channel-promoted fluorescent change of 21.<sup>33</sup> The addition of the peptide channels 1 and 3 indeed caused influx of  $\text{Na}^+$  cations from the external buffer and efflux of protons from the cells, leading to a pH change over time (Figure 4).<sup>34</sup> Higher efficiency of polytheonamide B 1 in the  $\text{H}^+/\text{Na}^+$  exchange in comparison to gramicidin D 3 correlated to more potent cytotoxicity of 1 (Table 1) as well as higher activity of 1 in the liposome experiments (Figure 2). In contrast, addition of strongly cytotoxic 6 did not affect the intracellular pH of the P388 cells. This result again indicated that the cytotoxicity of 6 was not induced by ion transport activity. The data in Figures 2 and 4 together corroborated that compound 6 exerted its cytotoxicity through a different mechanism of action from that

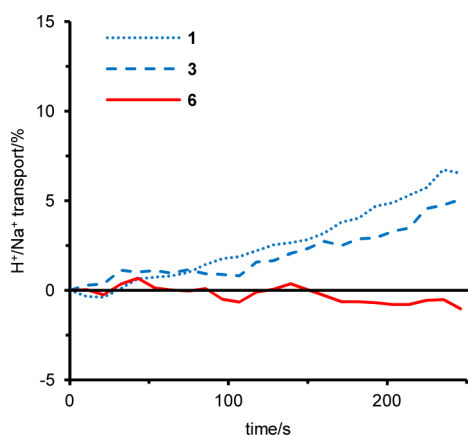


**Figure 4.** Time-course of  $H^+/Na^+$  exchange across cell membranes of the P388 leukemia cells caused by **1**, **3**, and **6**. Intracellular pH values were evaluated by the pH-dependent fluorescence of **21**. In all the experiments, peptides were added at 0 s.

of **1–3**, although **6** shares  $2/3$  of its sequence with ion-channel forming **2**.<sup>35</sup> Future detailed biological studies remain to be performed to determine this potential new mode of action of **6**.

In conclusion, we developed a unified and highly automated synthetic procedure for construction of the 13 substructures **4–16** of ion-channel forming dansylated polytheonamide mimic **2**, and we discovered that  $D,L$ -alternating 37-mer peptide **6** was more toxic than **2** and the other 12 substructures toward P388 mouse leukemia cells. Two types of functional assays of **6** revealed that **6** did not possess ion-channel activity, unlike polytheonamide B (**1**), the mimic **2**, and gramicidin D (**3**), suggesting that **6** exhibited its toxicity through a mode of action distinct from that of **1–3**. The discovery of **6** through structural permutations of polytheonamide B **1** demonstrates the benefits of total synthesis endeavors on complex molecule construction, and offers a unique opportunity for further exploration in chemical biology studies and drug discovery efforts. Detailed studies to elucidate its mode of action are currently underway in our laboratory.

## ■ ASSOCIATED CONTENT

### Supporting Information

Characterization data of all new compounds, synthetic procedures, assay data, and spectroscopic data. This material is available free of charge via the Internet at <http://pubs.acs.org>.

## ■ AUTHOR INFORMATION

### Corresponding Author

\*E-mail: [inoue@mol.f.u-tokyo.ac.jp](mailto:inoue@mol.f.u-tokyo.ac.jp).

### Funding

This work was supported financially by Funding Program for Next Generation World-Leading Researchers [Japan Society for the Promotion of Science (JSPS)] to M.I. The fellowship from JSPS to H.I. is gratefully acknowledged.

### Notes

The authors declare no competing financial interest.

## ■ ABBREVIATIONS

AM, acetoxymethylester; BCECF, 2',7'-bis(2-carboxyethyl)-5(6)-carboxyfluorescein; EYPC, egg yolk phosphatidylcholine; Fmoc, 9-fluorenylmethoxycarbonyl; HATU, *O*-(7-azabenzotriazole-1-yl)-*N,N,N',N'*-tetramethyluronium hexafluorophos-

phate; HEPES, 4-(2-hydroxyethyl)piperazine-1-ethanesulfonic acid; HOAt, 1-hydroxy-7-azabenzotriazole; MOPS, 3-morpholinopropanesulfonic acid; pyranine, trisodium 8-hydroxypyrene-1,3,6-trisulfonate; SAR, structure–activity relationship; *t*-Bu, *tert*-butyl; TFA, trifluoroacetic acid; Tmb, 2,4,6-trimethoxy benzyl; Tr, triphenylmethyl; XTT, 3'-[1-[(phenylamino)-carbonyl]-3,4-tetrazolium]bis(4-methoxy-6-nitro)-benzenesulfonic acid hydrate

## ■ REFERENCES

- (1) Hamada, T.; Matsunaga, S.; Yano, G.; Fusetani, N. Polytheonamides A and B, Highly Cytotoxic, Linear Polypeptides with Unprecedented Structural Features, from the Marine Sponge *Theonella swinhoei*. *J. Am. Chem. Soc.* **2005**, *127*, 110–118.
- (2) Hamada, T.; Sugawara, T.; Matsunaga, S.; Fusetani, N. Polytheonamides, Unprecedented Highly Cytotoxic Polypeptides, from the Marine Sponge *Theonella swinhoei*: 1. Isolation and Component Amino Acids. *Tetrahedron Lett.* **1994**, *35*, 719–720.
- (3) Hamada, T.; Matsunaga, S.; Fujiwara, M.; Fujita, K.; Hirota, H.; Schmucki, R.; Güntert, P.; Fusetani, N. Solution Structure of Polytheonamide B, a Highly Cytotoxic Nonribosomal Polypeptide from Marine Sponge. *J. Am. Chem. Soc.* **2010**, *132*, 12941–12945.
- (4) Iwamoto, M.; Shimizu, H.; Muramatsu, I.; Oiki, S. A Cytotoxic Peptide from a Marine Sponge Exhibits Ion Channel Activity through Vectorial-Insertion into the Membrane. *FEBS Lett.* **2010**, *584*, 3995–3999.
- (5) Oiki S.; Muramatsu I.; Matsunaga S.; Fusetani N. A Channel-Forming Peptide Toxin: Polytheonamide from Marine Sponge (*Theonella swinhoei*). *Folia Pharmacol. Jpn.* **1997**, *110* (Suppl. 1), 195–198.
- (6) Hotchkiss, R. D.; Dubos, R. J. Fractionation of the Bactericidal Agent from Cultures of a Soil *Bacillus*. *J. Biol. Chem.* **1940**, *132*, 791–792.
- (7) *Gramicidin and related ion channel-forming peptides*; Chadwick, D. J., Cardew, G., Eds.; Wiley & Sons: Chichester, 1999.
- (8) Inoue, M.; Shinohara, N.; Tanabe, S.; Takahashi, T.; Okura, K.; Itoh, H.; Mizoguchi, Y.; Iida, M.; Lee, N.; Matsuoka, S. Total Synthesis of the Large Non-Ribosomal Peptide Polytheonamide B. *Nat. Chem.* **2010**, *2*, 280–285.
- (9) Inoue, M. Total Synthesis and Functional Analysis of Non-Ribosomal Peptides. *Chem. Rec.* **2011**, *11*, 284–294.
- (10) Inoue, M.; Matsuoka, S. Convergent Total Synthesis of the Complex Non-Ribosomal Peptide Polytheonamide B. *Isr. J. Chem.* **2011**, *51*, 346–358.
- (11) Matsuoka, S.; Shinohara, N.; Takahashi, T.; Iida, M.; Inoue, M. Functional Analysis of Synthetic Substructures of Polytheonamide B: A Transmembrane Channel-Forming Peptide. *Angew. Chem., Int. Ed.* **2011**, *50*, 4879–4883.
- (12) Shinohara, N.; Itoh, H.; Matsuoka, S.; Inoue, M. Selective Modification of the N-Terminal Structure of Polytheonamide B Significantly Changes its Cytotoxicity and Activity as an Ion Channel. *ChemMedChem* **2012**, *7*, 1770–1773.
- (13) Itoh, H.; Matsuoka, S.; Kreir, M.; Inoue, M. Design, Synthesis and Functional Analysis of Dansylated Polytheonamide Mimic: An Artificial Peptide Ion Channel. *J. Am. Chem. Soc.* **2012**, *134*, 14011–14018.
- (14) Bollhagen, R.; Schmiedberger, M.; Barlos, K.; Grell, E. A New Reagent for the Cleavage of Fully Protected Peptides Synthesised on 2-Chlorotrityl Chloride Resin. *J. Chem. Soc., Chem. Commun.* **1994**, 2559–2560.
- (15) Barlos, K.; Chatzi, O.; Gatos, D.; Stavropoulos, G. 2-Chlorotrityl Chloride Resin. Studies on Anchoring of Fmoc-Amino Acids and Peptide Cleavage. *Int. J. Peptide Protein Res.* **1991**, *37*, 513–520.
- (16) *Fmoc Solid Phase Peptide Synthesis*; Chan, W. C., White, P. D., Eds.; Oxford University Press: New York, 2000.
- (17) Carpino, L. A. 1-Hydroxy-7-azabenzotriazole. An Efficient Peptide Coupling Additive. *J. Am. Chem. Soc.* **1993**, *115*, 4397–4398.



(18) Inverarity, I. A.; Hulme, A. N. Marked Small Molecule Libraries: A Truncated Approach to Molecular Probe Design. *Org. Biomol. Chem.* **2007**, *5*, 636–643.

(19) Tornøe, C. W.; Christensen, C.; Meldal, M. Peptidotriazoles on Solid Phase: [1,2,3]-Triazoles by Regiospecific Copper(I)-Catalyzed 1,3-Dipolar Cycloadditions of Terminal Alkynes to Azides. *J. Org. Chem.* **2002**, *67*, 3057–3064.

(20) Tron, G. C.; Pirali, T.; Billington, R. A.; Canonico, P. L.; Sorba, G.; Genazzani, A. A. Click Chemistry Reactions in Medicinal Chemistry: Applications of the 1,3-dipolar Cycloaddition Between Azides and Alkynes. *Med. Res. Rev.* **2008**, *28*, 278–308.

(21) Kolb, H. C.; Sharpless, K. B. The Growing Impact of Click Chemistry on Drug Discovery. *Drug Discovery Today* **2003**, *8*, 1128–1137.

(22) Kolb, H. C.; Finn, M. G.; Sharpless, K. B. Click Chemistry: Diverse Chemical Function from a Few Good Reactions. *Angew. Chem., Int. Ed.* **2001**, *40*, 2004–2021.

(23) Weygand, F.; Steglich, W.; Bjarnason, J. Leicht abspaltbare Schutzgruppen für die Säureamidfunktion, 3. Derivate des Asparagins und Glutamins mit 2.4-dimethoxy-benzyl- und 2.4.6-trimethoxy-benzylgeschützten Amidgruppen. *Chem. Ber.* **1968**, *101*, 3642–3648.

(24) Pearson, D. A.; Blanchette, M.; Baker, M. L.; Guindon, C. A. Trialkylsilanes as Scavengers for the Trifluoroacetic Acid Deblocking of Protecting Groups in Peptide Synthesis. *Tetrahedron Lett.* **1989**, *30*, 2739–2742.

(25) Scudiero, D. A.; Shoemaker, R. H.; Paull, K. D.; Monks, A.; Tierney, S.; Nofziger, T. H.; Currens, M. J.; Seniff, D.; Boyd, M. R. Evaluation of a Soluble Tetrazolium/Formazan Assay for Cell Growth and Drug Sensitivity in Culture Using Human and Other Tumor Cell Lines. *Cancer Res.* **1988**, *48*, 4827–4833.

(26) Roehm, N. W.; Rodgers, G. H.; Hatfield, S. M.; Glasebrook, A. L. An Improved Colorimetric Assay for Cell Proliferation and Viability Utilizing the Tetrazolium Salt XTT. *J. Immunol. Methods* **1991**, *142*, 257–265.

(27) Otis, F.; Racine-Berthiaume, C.; Voyer, N. How Far Can a Sodium Ion Travel within a Lipid Bilayer? *J. Am. Chem. Soc.* **2011**, *133*, 6481–6483.

(28) Clement, N. R.; Gould, J. M. Pyranine (8-Hydroxy-1,3,6-pyrenetrisulfonate) as a Probe of Internal Aqueous Hydrogen Ion Concentration in Phospholipid Vesicles. *Biochemistry* **1981**, *20*, 1534–1538.

(29) Membrane disruption also causes the fluorescent change in this liposome assay. A different set of experiments demonstrated that **1**, **2**, and **3** caused no membrane disruption, confirming that the fluorescent changes in Figure 2 were attributed to their potent ion transport activities. See refs 11 and 13.

(30) The 37 amino acid sequence from residues 12–48 of polytheonamide B **1** exhibited the potent H<sup>+</sup>/Na<sup>+</sup> ion exchange activity and the weak cytotoxic activity (IC<sub>50</sub> = 860 nM). Thus, the molecular behavior of **6** was also different from that of the corresponding substructure of **1**. See ref 11.

(31) The Stokes shift values of the dansyl groups of **2** (see ref 13) and **6** in liposomes were determined to be close to that in methanol and in buffer, respectively. The data indicated that the microenvironments of their residues were slightly different. See the Supporting Information for the details.

(32) Rink, T. J.; Tsien, R. Y.; Pozzan, T. Cytoplasmic pH and Free Mg<sup>2+</sup> in Lymphocytes. *J. Cell Biol.* **1982**, *95*, 189–196.

(33) The fluorescence intensity was converted to the intracellular pH values according to the calibration curve obtained by using ion transporter nigericin. See: Thomas, J. A.; Buchsbaum, R. N.; Zimniak, A.; Racker, E. Intracellular pH Measurements in Ehrlich Ascites Tumor Cells Utilizing Spectroscopic Probes Generated in Situ. *Biochemistry* **1979**, *18*, 2210–2218.

(34) Although the concentrations of the peptides (125 nM) were at least 10 times higher than their IC<sub>50</sub> values, the P388 cells were viable under these experimental conditions. This is because the cells were exposed to the peptides for a much shorter time (1.5 h) in comparison

to the cytotoxicity assay (4 days). See the Supporting Information for the experimental details.

(35) The CD spectrum of **6** in liposomes was found to be different from that of mimic **2**, suggesting the differences in their three-dimensional structures (see Figure S6 in the Supporting Information).